

Dirac Equation and Quantum Relativistic Effects in a Single Trapped Ion

L. Lamata,¹ J. León,¹ T. Schätz,² and E. Solano^{3,4}

¹*Instituto de Matemáticas y Física Fundamental, CSIC, Serrano 113-bis, 28006 Madrid, Spain*

²*Max-Planck-Institut für Quantenoptik, Hans-Kopfermann-Strasse 1, D-85748 Garching, Germany*

³*Physics Department, ASC, and CeNS, Ludwig-Maximilians-Universität, Theresienstrasse 37, 80333 Munich, Germany*

⁴*Sección Física, Departamento de Ciencias, Pontificia Universidad Católica del Perú, Apartado Postal 1761, Lima, Peru*

(Dated: November 26, 2024)

We present a method of simulating the Dirac equation in 3+1 dimensions for a free spin-1/2 particle in a single trapped ion. The Dirac bispinor is represented by four ionic internal states, and position and momentum of the Dirac particle are associated with the respective ionic variables. We show also how to simulate the simplified 1+1 case, requiring the manipulation of only two internal levels and one motional degree of freedom. Moreover, we study relevant quantum-relativistic effects, like the *Zitterbewegung* and Klein's paradox, the transition from massless to massive fermions, and the relativistic and nonrelativistic limits, via the tuning of controllable experimental parameters.

PACS numbers: 32.80.Pj, 03.67.-a, 03.65.Pm

The search for a fully relativistic Schrödinger equation gave rise to the Klein-Gordon and Dirac equations. P. A. M. Dirac looked for a Lorentz-covariant wave equation that is linear in spatial and time derivatives, expecting that the interpretation of the square wave function as a probability density holds. As a result, he obtained a fully covariant wave equation for a spin-1/2 massive particle, which incorporated *ab initio* the spin degree of freedom. It is known [1] that the Dirac formalism describes accurately the spectrum of the hydrogen atom and that it plays a central role in quantum field theory, where creation and annihilation of particles are allowed. However, the one-particle solutions of the Dirac equation in relativistic quantum mechanics predict some astonishing effects, like the *Zitterbewegung* and the Klein's paradox.

In recent years, a growing interest has appeared regarding simulations of relativistic effects in controllable physical systems. Some examples are the simulation of Unruh effect in trapped ions [2], the *Zitterbewegung* for massive fermions in solid state physics [3], and black-hole properties in the realm of Bose-Einstein condensates [4]. Moreover, the low-energy excitations of a nonrelativistic two-dimensional electron system in a single layer of graphite (graphene) are known to follow the Dirac-Weyl equations for massless relativistic particles [5, 6]. On the other hand, the fresh dialog between quantum information and special relativity has raised important issues concerning the quantum information content of Dirac bispinors under Lorentz transformations [7].

In this Letter, we propose the simulation of the Dirac equation for a free spin-1/2 particle in a single trapped ion. We show how to implement realistic interactions on four ionic internal levels, coupled to the motional degrees of freedom, so as to reproduce this fundamental quantum relativistic wave equation. We propose also the simulation of the Dirac equation in 1+1 dimensions, requiring only the control of two internal levels and one motional degree of freedom. We study some quantum-relativistic

effects, like the *Zitterbewegung* and the Klein's paradox, in terms of measurable observables. Moreover, we discuss the transition from massless to massive fermions, and from the relativistic to the nonrelativistic limit. Finally, we describe a possible experimental scenario.

We consider a single ion of mass M inside a Paul trap with frequencies ν_x , ν_y , and ν_z , where four metastable ionic internal states, $|a\rangle$, $|b\rangle$, $|c\rangle$, and $|d\rangle$, may be coupled pairwise to the center-of-mass (CM) motion in directions x , y , and z . We will make use of three standard interactions in trapped-ion technology, allowing for the coherent control of the vibronic dynamics [8]. First, a carrier interaction consisting of a coherent driving field acting resonantly on a pair of internal levels, while leaving untouched the motional degrees of freedom. It can be described effectively by the Hamiltonian $H_\sigma = \hbar\Omega(\sigma^+ e^{i\phi} + \sigma^- e^{-i\phi})$, where σ^+ and σ^- are the raising and lowering ionic spin-1/2 operators, respectively, and Ω is the associated coupling strength. The phases and frequencies of the laser field could be adjusted so as to produce $H_{\sigma_x} = \hbar\Omega_x \sigma_x$, $H_{\sigma_y} = \hbar\Omega_y \sigma_y$, and $H_{\sigma_z} = \hbar\Omega_z \sigma_z$, where σ_x , σ_y , and σ_z , are atomic Pauli operators in the conventional directions x , y , and z . Second, a Jaynes-Cummings (JC) interaction, usually called red-sideband excitation, consisting of a laser field acting resonantly on two internal levels and one of the vibrational CM modes. Typically, a resonant JC coupling induces an excitation in the internal levels while producing a deexcitation of the motional harmonic oscillator, and viceversa. The resonant JC Hamiltonian can be written as $H_r = \hbar\eta\tilde{\Omega}(\sigma^+ a e^{i\phi_r} + \sigma^- a^\dagger e^{-i\phi_r})$, where a and a^\dagger are the annihilation and creation operators associated with a motional degree of freedom. $\eta = k\sqrt{\hbar/2M\nu}$ is the Lamb-Dicke parameter [8], where k is the wave number of the driving field. Third, an anti-JC (AJC) interaction, consisting of a JC-like coupling tuned to the blue motional sideband with Hamiltonian $H_b = \hbar\eta\tilde{\Omega}(\sigma^+ a^\dagger e^{i\phi_b} + \sigma^- a e^{-i\phi_b})$. In this case, an in-

ternal level excitation accompanies an excitation in the considered motional degree of freedom, and viceversa.

All these interactions could be applied simultaneously and addressed to different pairs of internal levels coupled to different CM modes. For example, it is possible to adjust field phases to implement a simultaneous blue and red sideband excitation scheme to form the Hamiltonian $H_{\sigma_x}^{p_x} = i\hbar\eta_x\tilde{\Omega}_x\sigma_x(a_x^\dagger - a_x) = 2\eta_x\Delta_x\tilde{\Omega}_x\sigma_x p_x$, with $i(a_x^\dagger - a_x)/2 = \Delta_x p_x/\hbar$. Here, $\Delta_x := \sqrt{\hbar/2M\nu_x}$ is the spread in position along the x -axis of the zero-point wavefunction and p_x the corresponding dimensioned momentum operator. The physics of $H_{\sigma_x}^{p_x}$ cannot be described anymore by Rabi oscillations. In turn, it yields a conditional displacement in the motion depending on the internal state, producing the so-called Schrödinger cat states [9, 10]. By further manipulation of laser field directions and phases, we can also implement $H_{\sigma_y}^{p_y} = 2\eta_y\Delta_y\tilde{\Omega}_y\sigma_y p_y$ and $H_{\sigma_z}^{p_z} = 2\eta_z\Delta_z\tilde{\Omega}_z\sigma_z p_z$. This kind of interactions has already been produced in the lab, under resonant [11] and dispersive conditions [12].

We define the wave vector associated with the four ionic internal levels as

$$|\Psi\rangle := \Psi_a|a\rangle + \Psi_b|b\rangle + \Psi_c|c\rangle + \Psi_d|d\rangle = \begin{pmatrix} \Psi_a \\ \Psi_b \\ \Psi_c \\ \Psi_d \end{pmatrix}. \quad (1)$$

We may apply simultaneously different laser pulses, with proper directions and phases, $\eta \equiv \eta_x = \eta_y = \eta_z$, $\Delta \equiv \Delta_x = \Delta_y = \Delta_z$, $\tilde{\Omega} \equiv \tilde{\Omega}_x = \tilde{\Omega}_y = \tilde{\Omega}_z$, $\Omega \equiv \Omega_x = \Omega_y = \Omega_z$, to compose the following Hamiltonian acting on $|\Psi\rangle$,

$$H_D = 2\eta\Delta\tilde{\Omega}(\sigma_x^{ad} + \sigma_x^{bc})p_x + 2\eta\Delta\tilde{\Omega}(\sigma_y^{ad} - \sigma_y^{bc})p_y + 2\eta\Delta\tilde{\Omega}(\sigma_x^{ac} - \sigma_x^{bd})p_z + \hbar\Omega(\sigma_y^{ac} + \sigma_y^{bd}). \quad (2)$$

We rewrite Eq. (2) in the suitable matrix form

$$H_D = \begin{pmatrix} 0 & 2\eta\Delta\tilde{\Omega}(\vec{\sigma} \cdot \vec{p}) - i\hbar\Omega \\ 2\eta\Delta\tilde{\Omega}(\vec{\sigma} \cdot \vec{p}) + i\hbar\Omega & 0 \end{pmatrix}, \quad (3)$$

where each entry represents a 2×2 matrix. The associated Schrödinger equation, $H_D|\Psi\rangle = i\hbar\partial|\Psi\rangle/\partial t$, performs the same dynamics as the *Dirac equation* in 3+1 dimensions for a free spin-1/2 particle, where $|\Psi\rangle$ represents the four-component Dirac bispinor. This is easily seen if we express the Dirac equation

$$i\hbar\frac{\partial\psi}{\partial t} = \mathcal{H}_D\psi = (c\vec{\alpha} \cdot \vec{p} + \beta mc^2)\psi \quad (4)$$

in its ‘‘supersymmetric’’ representation [1]

$$\mathcal{H}_D = \begin{pmatrix} 0 & c(\vec{\sigma} \cdot \vec{p}) - imc^2 \\ c(\vec{\sigma} \cdot \vec{p}) + imc^2 & 0 \end{pmatrix}. \quad (5)$$

Here, the 4×4 matrix $\vec{\alpha} := (\alpha_x, \alpha_y, \alpha_z) = \text{off-diag}(\vec{\sigma}, \vec{\sigma})$ is the velocity operator, $\beta := \text{off-diag}(-i\mathbb{1}_2, i\mathbb{1}_2)$, and

$$c := 2\eta\Delta\tilde{\Omega}, \quad mc^2 := \hbar\Omega, \quad (6)$$

are the speed of light and the electron rest energy, respectively. The notorious analogy between Eqs. (3) and (5) shows that the quantum relativistic evolution of a spin-1/2 particle can be fully reproduced in a tabletop ion-trap experiment, allowing the study of otherwise unaccessible physical regimes and effects, as shown below.

In the Dirac formalism, the spin-1/2 degree of freedom is incorporated *ab initio*. Moreover, the Dirac bispinor in Eq. (1) is built by components associated with positive and negative energies, $E_D^\pm = \pm\sqrt{p^2c^2 + m^2c^4}$. This description is the source of diverse controversial predictions, as the *Zitterbewegung* and the Klein’s paradox.

The *Zitterbewegung* is a known quantum-relativistic effect consisting of a *helical motion of a free Dirac particle*, a natural consequence of the non-commutativity of its velocity operator components, $c\alpha_i$, with $i = x, y, z$. It can be proved straightforwardly [1] that the time evolution of the position operator $\vec{r} = (x, y, z)$ in the Heisenberg picture, following $d\vec{r}/dt = [\vec{r}, H_D]/i\hbar$, reads

$$\vec{r}(t) = \vec{r}(0) + \frac{4\eta^2\Delta^2\tilde{\Omega}^2\vec{p}}{H_D}t + \left(\vec{\alpha} - \frac{2\eta\Delta\tilde{\Omega}\vec{p}}{H_D}\right)\frac{i\hbar\eta\Delta\tilde{\Omega}}{H_D}\left(e^{2iH_D t/\hbar} - 1\right). \quad (7)$$

Here, the first two terms on the r.h.s. account for the classical kinematics of a free particle, while the last oscillating term is responsible for a transversal ‘‘quivering’’ motion. If we consider a bispinor state with a peaked momentum around p_0 , $|\Psi_0\rangle = |a\rangle \otimes \exp[-(p-p_0)^2/2\sigma_p^2]$, the *Zitterbewegung* frequency associated with the measurable quantity $\langle\vec{r}(t)\rangle$ can be estimated as

$$\omega_{ZB} \approx 2|\bar{E}_D|/\hbar \equiv 2\sqrt{4\eta^2\Delta^2\tilde{\Omega}^2p_0^2/\hbar^2 + \Omega^2} \approx 2\sqrt{N\eta^2\tilde{\Omega}^2 + \Omega^2}, \quad (8)$$

where $\bar{E}_D \equiv \langle H_D \rangle$ and $N \equiv \langle a^\dagger a \rangle$ are the average energy and phonon number, respectively. Similarly, we can estimate from Eq. (7) the *Zitterbewegung* amplitude associated with $\langle\vec{r}(t)\rangle$ as

$$R_{ZB} = \frac{\hbar}{2mc} \left(\frac{mc^2}{E}\right)^2 = \frac{\eta\hbar^2\tilde{\Omega}\Omega\Delta}{4\eta^2\tilde{\Omega}^2\Delta^2p_0^2 + \hbar^2\Omega^2}, \quad (9)$$

and $R_{ZB} \approx \Delta$, if $\eta\tilde{\Omega} \sim \Omega$.

The standard explanation of this erratic motion for a free Dirac particle invokes the interference between the positive- and negative-energy components of the Dirac bispinor following the dynamics in Eqs. (3) and (5). The predicted values for a real electron, $\omega_{ZB} \sim 10^{21}\text{Hz}$ and $R_{ZB} \sim 10^{-3}\text{\AA}$, are out of experimental reach, the effect has never been observed, and its existence is even questioned by quantum field theory considerations. To simulate quantum-relativistic effects in other physical systems, like trapped ions or graphene, is not aimed at proving their existence, but at exploiting the differences and

analogies in each field. Given the flexibility of trapped-ion systems, we will have access to a wide range of tunable experimental parameters [8], allowing for realistic and measurable $\omega_{\text{ZB}} \sim 0 - 10^6 \text{ Hz}$ and $R_{\text{ZB}} \sim 0 - 10^3 \text{ \AA}$, depending on the initial vibronic states. Due to our piecewise build-up of the 3+1 Dirac Hamiltonian of Eq. (2), we can strongly reduce the experimental demands to study Dirac equations in 1+1 and 2+1 dimensions [1, 13]. In those cases, the Clifford algebra that characterizes the Dirac matrices is satisfied by the anticommuting Pauli matrices, $\{\sigma_i, \sigma_j\} = 2\delta_{ij}$, where $\{A, B\} := AB + BA$, given that we only need 2(3) anticommuting matrices in the 1+1(2+1) case. Accordingly, the four components of the Dirac bispinor are conveniently reduced to only two.

We focus now on the 1+1 dimensional case, which could be reached by current experiments, keeping most striking results available. After a unitary transformation around the x -axis, transforming σ_y into σ_z , the 1+1 Dirac equation stemming from Eq. (2) can be cast into $i\hbar\partial|\Psi^{(1)}\rangle/\partial t = H_{\text{D}}^{(1)}|\Psi^{(1)}\rangle$ with

$$\begin{aligned} H_{\text{D}}^{(1)} &= i\hbar\eta\tilde{\Omega}\sigma_x(a_x^\dagger - a_x) + \hbar\Omega\sigma_z \\ &\equiv 2\eta\Delta\tilde{\Omega}\sigma_x p_x + \hbar\Omega\sigma_z, \end{aligned} \quad (10)$$

where the Dirac ‘‘spinor’’ $|\Psi^{(1)}\rangle = \Psi_a^{(1)}|a\rangle + \Psi_b^{(1)}|b\rangle$. Note that these two components are not associated with the spin-1/2 degree of freedom but are linear combinations of positive- and negative-energy solutions [13]. Our setup is now reduced to a simultaneous JC + AJC interaction, $\sigma_x p_x$, and a Stark-shift term σ_z acting on two internal levels. In Eq. (10), the use of σ_z is for the sake of pedagogy, and returning to σ_y will not affect the results.

In the nonrelativistic limit, $mc^2 \gg p_x c$, or equivalently $\Omega \gg \eta\tilde{\Omega}$, we may identify the dispersive limit in Eq. (10), and derive the *squeezing* second-order Hamiltonian

$$H_{\text{eff}}^{(1)} = \frac{2\eta^2\Delta^2\tilde{\Omega}^2}{\hbar\Omega}\sigma_z p_x^2 \equiv \sigma_z \frac{p_x^2}{2m}, \quad (11)$$

yielding the expected Schrödinger Hamiltonian associated with the classical kinetic energy of a free particle. In the relativistic limit, $mc^2 \ll p_x c$, which includes $m = 0$, the 1+1 case reduces to $H_{\text{D}}^{(1)} = i\hbar\eta\tilde{\Omega}\sigma_x(a_x^\dagger - a_x)$, which produces Schrödinger cats, as commented above [9, 10].

For a massless particle, we can show that $dx/dt = [x, H_{\text{D}}^{(1)}]/i\hbar = 2\eta\Delta\tilde{\Omega}\sigma_x$ and $d\sigma_x/dt = [\sigma_x, H_{\text{D}}^{(1)}]/i\hbar = 0$. In consequence, σ_x is a constant of motion and the time evolution of the position operator,

$$x(t) = x(0) + 2\eta\Delta\tilde{\Omega}\sigma_x t, \quad (12)$$

is classical and does not involve *Zitterbewegung*. On the other hand, for a massive particle, $d\sigma_x/dt = [\sigma_x, H_{\text{D}}]/i\hbar = -\Omega\sigma_y$, $d\sigma_y/dt \neq 0$, and so forth. The produced set of differential equations yields a *Zitterbewegung* oscillatory solution similar to Eq. (7), with the evident simplification via the replacements of H_{D} by $H_{\text{D}}^{(1)}$,

\vec{p} by p_x , and $\vec{\alpha}$ by σ_x . It is noteworthy to mention that the phenomenon of mass acquisition, which could be done here in a continuous manner by raising the coupling strength Ω , is related to the spontaneous symmetry breaking mechanism of the Higgs field.

At this stage, it is clear that the measurement of the expectation value of the position operator, $\langle x(t) \rangle$, as a function of the interaction time t is of importance. A recent proposal for realizing fast measurements of motional quadratures [14] relies on the possibility of measuring the population of an ionic internal level, P_a , at short probe-motion interaction times τ with high precision [15]. Given an initial vibronic state $\rho(0) = |+\phi\rangle\langle+\phi| \otimes \rho_m$, where $|\pm\phi\rangle = (|a\rangle \pm e^{i\phi}|b\rangle)/\sqrt{2}$ and ρ_m describes an unknown motional density operator, we can make use of

$$\langle Y_\phi \rangle = \frac{d}{d\tau} P_e^{+\phi}(\tau) \Big|_{\tau=0}, \quad (13)$$

where the generalized quadrature $Y_\phi = (ae^{-i\phi} - a^\dagger e^{i\phi})/2i$. Then, position and momentum operators are measured when choosing $\phi = -\pi/2$ and $\phi = 0$, respectively. To apply this technique, it is required a particular initial state of the internal states, so the measurement of $\langle x(t) \rangle$ would have to be done in two parts, one associated with each of the suitably projected states, $|+\phi\rangle$ and $|-\phi\rangle$.

We turn now to the possible simulation of Klein’s paradox. In 1929, Klein noticed [16] the anomalous behavior of Dirac particles in regions where a high potential energy V exists: $H_V^{(1)} = H_{\text{D}}^{(1)} + V\mathbb{1}_2$. When $V > 2mc^2$, negative-energy electrons (components) may swallow V , acquiring positive energy and behaving as ordinary electrons, while leaving a hole in the Dirac sea. This stems from the fact that the relativistic energy related to $H_V^{(1)}$ may be recast into $(pc)^2 = (E_V^{(1)} - V + mc^2)(E_V^{(1)} - V - mc^2)$, which is positive when either both factors are positive or negative. In the second case, the total energy $E_V^{(1)} < -mc^2 + V$ can be larger than mc^2 , as noticed by Klein. In this case an $e^- - e^+$ (electron-positron) pair could be created from V . The sudden raise of the constant potential $V(|a\rangle\langle a| + |b\rangle\langle b|)$, at a certain time $t = t_0$ after an evolution associated with $H_{\text{D}}^{(1)}$, could simulate this phenomenon. We suggest to produce potential V with the required characteristics through a fast and homogeneous Stark shift in both internal levels. The natural way to detect Klein’s paradox, assuming an initial positive-energy internal state $|a\rangle$ ($p_0 = 0$), is via measurement of nonzero population in the negative-energy component $|b\rangle$.

Finally, in as much as massless chiral fermions in condensed matter, we could also produce a 1+1 axial anomaly [17] by changing Eq. (10) into $H_{\text{D}}^{(1)} = c\sigma_x p_x + qEx$, where $x \propto (a + a^\dagger)$ is a motional displacement.

The basic ingredients to implement the 1D Dirac dynamics of Eq. (10) with a single trapped ion are two independent electronic (internal) states coupled to a one-dimensional motional degree of freedom. The required

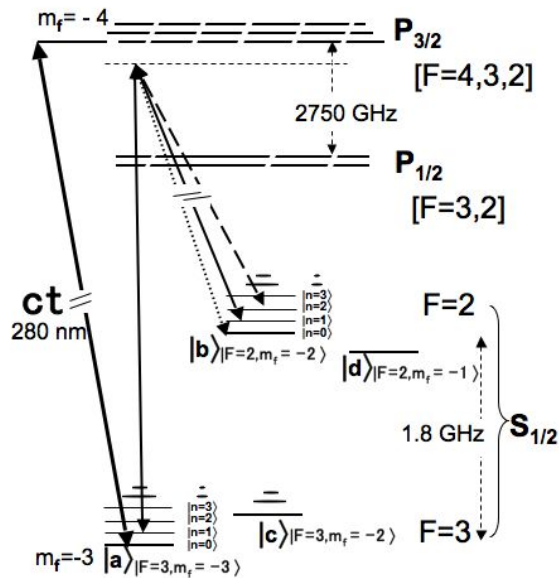


FIG. 1: Relevant energy levels (not to scale) of a $^{25}\text{Mg}^+$ ion. Shown are the ground-state hyperfine levels supplying the two internal states, $|a\rangle$ and $|b\rangle$, and the equidistant harmonic oscillator levels related to the harmonic axial confinement in a trap similar to that described in [18, 19]. We subsumed excited levels of the $P_{1/2}$ and $P_{3/2}$ states. We depict the resonant transition state sensitive detection and the relevant types of two photon stimulated Raman transitions between states $|a, n=1\rangle$ and $|b, n=0,1,2\rangle$: red sideband (dotted line), carrier (solid line), and blue sideband (dashed line).

states could be composed by two ground-state hyperfine levels of an earth alkaline atomic ion, e.g. of $^{25}\text{Mg}^+$ by $|F=3; m_f=-3\rangle$ and $|F=2; m_f=-2\rangle$, $|a\rangle$ and $|b\rangle$, respectively, as depicted in Fig. 1. A constant external magnetic field will define the quantization axis and lift the degeneracy of levels being potentially useful to provide additional states (like $|c\rangle$ and $|d\rangle$ in Fig. 1) necessary for higher dimensional simulations, see Eq. (2).

At the start, the ions will be laser cooled close to the motional ground state and optically pumped into state $|a\rangle$ [20]. One red/blue sideband and one carrier transition will be driven simultaneously [11, 21] to implement the desired dynamics of Eq. (5) via two-photon stimulated Raman transitions. To measure the ion position we rely on the mapping of motional information on the internal degrees of freedom [14, 15] and take advantage of the high fidelity of state sensitive detection realized by an additional laser beam, tuned to a cycling transition [22], coupling state $|a\rangle$ resonantly to the $P_{3/2}$ level. Considering the available laser intensities [23], all necessary Raman beams could be derived from a single laser source. We split the original beam and provide the necessary frequency offsets, phase control and switching via multi-passing through Acusto-Optical-

Modulators [21]. The number of laser beams could be further reduced by electro optical modulators to provide red and blue sidebands simultaneously [11, 12]. To implement an overall shift in the potential (Stark shift of level $|a\rangle$ and $|b\rangle$ in Klein's paradox) without changing their mutual energy difference we chose the directions and polarizations of the Raman beams appropriately.

In conclusion, we have shown how to simulate the Dirac equation in 3+1 dimensions for a free spin-1/2 particle, and quantum-relativistic effects like the *Zitterbewegung* and Klein's paradox, in a single trapped ion. We have studied the 1+1 case, where experimental needs are minimal while keeping most striking predictions. We believe that these simulations open attractive avenues and a fruitful dialog between different scientific communities.

The authors thank D. Leibfried and J. I. Latorre for valuable comments. L.L. acknowledges support from MEC FPU grant No. AP2003-0014. L.L. and J.L. were partially supported by the Spanish MEC FIS2005-05304 and CSIC 2004 5 0E 271 projects. T.S. acknowledges support by DFG, MPQ, and MPG. E.S. is grateful for the hospitality at CSIC (Madrid) and acknowledges support from EU EuroSQIP and DFG SFB 631 projects.

-
- [1] B. Thaller, *The Dirac Equation* (Springer-Verlag, Berlin 1992).
 - [2] P.M. Alsing, J.P. Dowling, and G.J. Milburn, Phys. Rev. Lett. **94**, 220401 (2005).
 - [3] J. Schliemann, D. Loss, and R.M. Westervelt, Phys. Rev. Lett. **94**, 206801 (2005).
 - [4] L. J. Garay *et al.*, Phys. Rev. Lett. **85**, 4643 (2000).
 - [5] J. Cserti and G. Dávid, Phys. Rev. B **74**, 172305 (2006).
 - [6] M. I. Katsnelson, K. S. Novoselov, and A. K. Geim, Nature Phys. **2**, 620 (2006).
 - [7] A. Peres and D. R. Terno, Rev. Mod. Phys. **76**, 93 (2004).
 - [8] D. Leibfried *et al.*, Rev. Mod. Phys. **75**, 281 (2003).
 - [9] E. Solano, R. L. de Matos Filho, and N. Zagury, Phys. Rev. Lett. **87**, 060402 (2001).
 - [10] E. Solano, G.S. Agarwal, and H. Walther, Phys. Rev. Lett. **90**, 027903 (2003).
 - [11] P.C. Haljan *et al.*, Phys. Rev. Lett. **94**, 153602 (2005).
 - [12] C. A. Sackett *et al.*, Nature (London) **404**, 256 (2000).
 - [13] B. Thaller, quant-ph/0409079.
 - [14] P. Lougovski, H. Walther, and E. Solano, Eur. Phys. J. D **38**, 423 (2006).
 - [15] D. M. Meekhof *et al.*, Phys. Rev. Lett. **76**, 1796 (1996).
 - [16] O. Klein, Z. Phys. **53**, 157 (1929).
 - [17] H. B. Nielsen and M. Ninomiya, Phys. Lett. **130** B, 389 (1983).
 - [18] M. A. Rowe *et al.*, Quantum Inf. Comput. **2**, 257 (2002).
 - [19] F. Schmidt-Kaler *et al.*, Appl. Phys. B **77**, 789 (2003).
 - [20] B. E. King *et al.*, Phys. Rev. Lett. **81**, 1525 (1998).
 - [21] D. J. Wineland *et al.*, Phil. Trans. Royal Soc. London A **361**, 1349 (2003).
 - [22] C. Monroe *et al.*, Phys. Rev. Lett. **75**, 4714 (1995).
 - [23] A. Friedenauer *et al.*, Appl. Phys. B **84**, 371 (2006).